



Numerical analysis of the breakwater failure at the Sergipe Terminal Port

Pedro Oliveira Bogossian Roque^{1#} , Celso Romanel¹ ,

Celso Antero Ivan Salvador Villalobos¹ , Jackeline Castañeda Huertas¹ 

Article

Keywords

Numerical analysis
Embankment on soft soils
Incremental construction
Breakwater
Slope failure

Abstract

The breakwater failure at the Sergipe Harbor is a well-known event among the Brazilian geotechnical community, which provided great knowledge about the behavior of embankments on soft soils, although some questions still remain, since the back analysis diverged from the field outcome. In this context, this work aims to carry out a numerical analysis of the construction of the breakwater using the finite element method to understand the mechanisms of failure. A fully coupled flow-deformation analysis was performed in Plaxis 2D software, using the Soft Soil Creep and Mohr-Coulomb constitutive soil models. The Volume Method was also applied to estimate the stability of the slopes, from the calculated numerical displacements. The interpretation of the results allowed to verify that the analysis simulated behaviors that had been raised as responsible for the failure. High excess pore pressure levels were generated in the phase at which failure occurred, in addition to a strain softening behavior, which, alongside the progressive failure, could justify why the back analysis considering unrealistic gains in undrained strength, calculated by the increase of the vertical effective stresses, had provided missed factors of safety. Although shear deformations and horizontal displacements were verified for both sides of the breakwater, the “shared failure” assumption could not be verified, since the shear stress was mobilized in the rockfill.

1. Introduction

The failure of the Sergipe Port Terminal (TPS) breakwater is one of the most well-known events among the Brazilian geotechnical community. Occurred in the late 1980s, the case was the subject of several works published in the national and international literature, discussing both the foundation slide failure in the initial design of the rockfill structure (Sandroni et al., 2018) as well as the modeling of the redesigned TPS (Brugger et al., 1998) constructed in the early years of 1990s. The rockfill structure, composed of a geotechnical berm 5.0 m thick and a hydraulic berm, was intended to protect the port pier, located more than 2.0 km from the shore, due to the large volume of sediment carried along the beach, and was placed on a soil profile with a surface layer of sand over a deposit of 7.0 m of soft soil (Figure 1).

The construction of the geotechnical berm was carried out with a side dump vessel from the temporary loading port. After an interval of about 6 months due to weather conditions, the construction of the hydraulic berm was started in August

1989 from the access bridge to the breakwater and, on October 12th of the same year, it failed. Studying the accident provided a great deal of learning about the construction of embankments on soft soils. However, despite the knowledge acquired, some doubts about the failure of the breakwater’s original design remained, since the back analyses carried out both in terms of total and effective stresses, resulted in Factors of Safety greater than unity.

Some hypotheses were raised to explain the event such as: (a) the occurrence of progressive rupture in the soft clay, with loss of post-peak resistance and redistribution of shear stresses; (b) developing of excess pore pressure along the failure surface, reducing the effective acting stresses; (c) the occurrence of the shared failure phenomenon, based on the shear strength has not been completely developed in the rockfill body due to the failure mechanism.

Thus, the main objective of this work is to carry out a numerical back-analysis using the finite element method (FEM) to understand the mechanisms that led the breakwater of the TPS to rupture.

[#]Corresponding author. E-mail address: pedro_roque_93@yahoo.com.br

¹Pontifícia Universidade Católica do Rio de Janeiro, Departamento de Engenharia Civil e Ambiental, Rio de Janeiro, RJ, Brasil.

Submitted on May 15, 2023; Final acceptance on October 25, 2023; Discussion open until February 28, 2024.

<https://doi.org/10.28927/SR.2023.005223>



This is an Open Access article distributed under the terms of the Creative Commons Attribution License, which permits unrestricted use, distribution, and reproduction in any medium, provided the original work is properly cited.

To reach the proposed objective, a study was carried out using the finite element software for geotechnical problems Plaxis 2D v2020 considering a fully coupled flow-deformation analysis, using both the Soft Soil Creep (SSC) and the Mohr-Coulomb (MC) models in the soft clay layer of the foundation. The parameters used in the analyses were estimated based on the interpretation of geotechnical field and laboratory investigations in the foundation of the breakwater.

Additionally, an assessment of the stability of the breakwater was carried out using the Volume Method (Sandroni et al., 2004) based on the results of vertical and horizontal displacements obtained from the FEM analyses.

2. Geotechnical characteristics of Sergipe’s soft soil

The breakwater was built over a four-meter surface sand layer, with SPT blow count (N_{SPT}) from 6 to 15 blows/30 cm on a 7-meter layer of very soft clay. Below the clay layer, there were clayey sand and sandy clay deposits, with N_{SPT} increasing with depth (Figure 2). This profile had great lateral homogeneity throughout the entire area of the work. To characterize the materials, notably the soft clay layer, several test campaigns were carried out by different institutions, many of them were published in the technical literature (Ladd & Lee, 1993; Sandroni et al., 1997; Brugger, 1996).

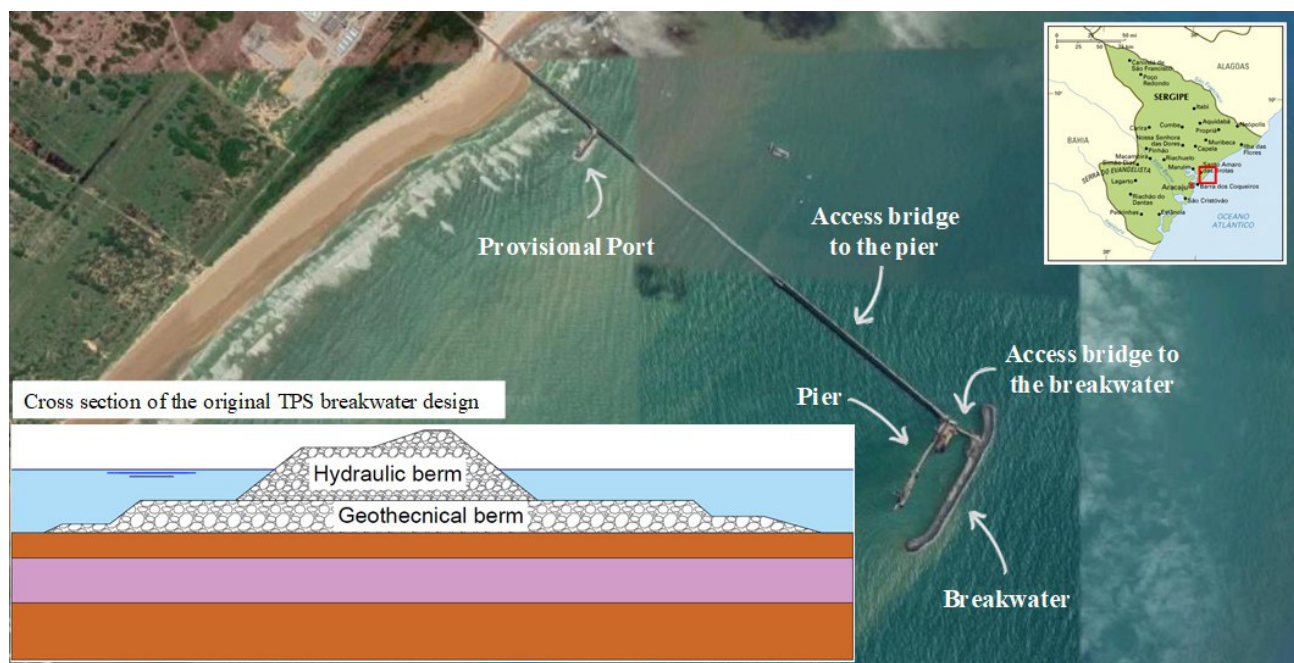


Figure 1. Location and typical cross-section of the original TPS breakwater design.

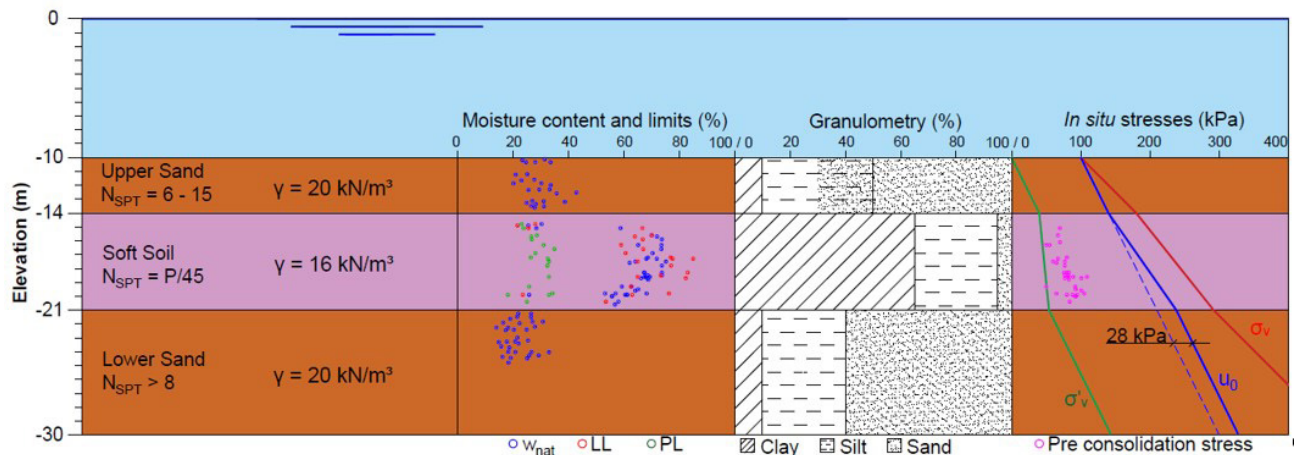


Figure 2. Typical stratigraphy of the TPS breakwater foundation materials showing variation of moisture content (w_{nat}), liquidity limit (LL), plasticity limit (PL), granulometry, in situ stresses and pre-consolidation stress.

According to the characterization process, the sand layers had a moisture content w_{nat} between 20 and 30% and the soft clay had an average moisture content between 54 and 72%, a plasticity limit PL between 24 and 35% and a liquidity limit LL between 58 and 85% (Ribeiro, 1992), although at some points LL was greater than 1.0, which could explain a metastable behavior of the soft clay (Sandroni et al., 1997).

Field geotechnical investigations, as well as piezometers installed in the clay, indicated a probable artesianism of approximately 28 kPa due to a freshwater aquifer in the lower sand layer, confined by the low permeability clay layer. This condition would be causing an upward freshwater flow in the clay, inducing the leaching of salts in its pores, in addition to reducing the effective stresses and increasing the sensitivity of the material.

Consolidation tests allowed verifying the Sergipe clay slightly pre-consolidated condition ($1 < OCR < 2$), with higher OCR at the top, lower between -16.0 m and -1.0 m elevations and then increasing with depth, indicating that artesianism dates to a geological age after the deposition of the material.

To determine the strength parameters of the clay, both field tests (vane tests and piezocone) and special laboratory tests (triaxial CIU and CK_0U and direct single shear tests DSS) results were evaluated. For laboratory tests with axial compression path, the values of undrained shear resistance as a function of the confining stress were equal to 0.30 for the CIU test, 0.24 for the CK_0U test and 0.22 for the DSS test. In the stress paths of the compression triaxial tests, the Skempton pore water pressure parameter A was greater than 1.0, confirming the sensitivity of the material.

The results of the Vane Tests indicated an increasing Su_{VT} profile with depth, with values close to 15 kPa at the top of the clay and reaching about 25 kPa at the base of the layer. These values do not consider the Bjerrum (1973) correction factor (μ), equal to 0.8 for Sergipe's clay (Sandroni, 2012 apud Schnaid & Odebrecht, 2012). The results of the CPTu tests allowed the construction of the N_{KT} profile, decreasing with depth, ranging from 16 at the top to 12 at the bottom (Brugger, 1996; Sandroni et al., 1997).

Based on the results of oedometric consolidation tests, it was also possible to define profiles of initial void ratios (e_0), compression (C_c) and swelling (C_s) indexes as a function of depth. The interpretation of the results were made by Geoprojetos (1992), Ladd & Lee (1993) and Brugger (1996), the last one adopted as initial values for the interactive process during the numerical analysis of the present research.

3. Numerical simulation of the construction of the breakwater

3.1 Finite element method

The numerical simulation of the rupture of the TPS breakwater was performed using the Plaxis 2D v.2020 software

based on the Finite Element Method (FEM). The problem was represented in the plane strain state and discretized into 15-node triangular finite elements, automatically generated by the program with mesh refinement optimization.

The constructive sequence was adopted according to the time-path diagram of the construction stages presented by Sandroni (2016). The loading and consolidation of the geotechnical berm totaled 175 days. Loading the hydraulic berm took 55 days and was divided into 8 phases in the simulation. The loading phases were of the fully coupled flow and deformation type, used when there is a need to simultaneously evaluate the evolution of deformations and pore pressures in saturated or partially saturated soils.

The breakwater foundation clay was divided into 7 sublayers of 1.0 m thick each and represented using both the Mohr-Coulomb (MC) and the Soft Soil Creep (SSC) models. This distinction was necessary since, in the SSC model, undrained analysis is available only in terms of effective stresses.

For the analysis in terms of total stresses, the values of Su of the vane test were adopted with and without Bjerrum correction, with and without a resistance gain due to the loading of the geotechnical berm. The gain was calculated as a function of the variation of the effective vertical stresses calculated from the analysis and evolution of the steps of the numerical model.

The SSC model is applied to soft soils of high compressibility, suitable for compressive stress paths, as is the case of embankment construction. The model is a variation of the Soft Soil model, which is based on the Modified Cam-Clay model considering a logarithmic relationship between the mean effective stress p' and the volumetric strain instead of the void ratio.

Table 1 presents the geotechnical parameters considered for the clay sublayers based on the results of field and laboratory tests, where c_k represents the variation of the initial vertical permeability coefficient k_{v0} with the void ratio. It was also assumed, based on field and laboratory tests, a horizontal anisotropy ratio $k_h/k_v = 2$. The value of ϕ_{cv} was determined by means of analysis of stress versus deformation curves determined in COPPE and PUC-Rio laboratory tests. An attempt was made to obtain agreement between the experimental curves and the model's theoretical curves by calibrating the curves using the SoilTest tool in Plaxis 2D, finally obtaining the value $\phi_{cv} = 18^\circ$.

Sand and rockfill layers were simulated using the MC model. For the cohesionless sand layers, the saturated unit weight γ_{sat} was 20 kN/m³ and the permeability coefficient k was 10⁻⁶ m/s. The effective friction angle ϕ' adopted for the upper sand layer was equal to 32° and for the lower sand layer it was equal to 35°. For the rockfill, γ_{sat} was 18 kN/m³ and ϕ' was 51°.

3.2 Volume method

The Volume Method (Sandroni et al., 2004) is an empirical method for evaluating the stability of embankments executed on soft soils based on variations of volume of vertical and horizontal displacements, ΔV_v and ΔV_h , measured during construction.

Due to the lack of field records, in this research the numerical displacements were applied, assuming them to be representative of the field conditions. The basic criterion of the method proposes that:

- $\Delta V_v / \Delta V_h > 6$ for stable condition.
- $3 \leq \Delta V_v / \Delta V_h \leq 6$ for the intermediate condition of stability.
- $\Delta V_v / \Delta V_h < 3$ for unstable condition.

Figure 3 shows a schematic representation of the volumes of vertical and horizontal displacements, for both sides (sea and coast) of the TPS breakwater. The parameter $\beta = V_{h1} / V_{h2}$, defined as the ratio between the volumes of horizontal displacements towards the side of the sea (V_{h1}) and towards the side of the coast (V_{h2}), was numerically calculated from the FEM analysis. This parameter thus enables the estimation of the volumes of vertical displacements for each side of the breakwater, in each of the loading phases, according to Equations 1 and 2.

$$V_{v1} = \frac{V_v \beta}{(1 + \beta)} \tag{1}$$

$$V_{v2} = \frac{V_v}{(1 + \beta)} \tag{2}$$

Although Equations 1 and 2 were proposed by Sandroni et al. (2004) for cases in which there is variation

in the width of the berm only, the volume method has been applied to situations considering the variation of the height of the embankment also (Dienstmann, 2011; Cobe, 2017; Sandroni et al., 2018; Cordeiro, 2019).

4. Analysis and results

4.1 Finite element method

4.1.1 Vertical displacements

Figure 4 presents the calculated vertical displacements along the base of the breakwater in each of the phases of the numerical simulation.

It is possible to observe a gradual increase in vertical displacements at the base of the breakwater with increasing its height. In Phase 10 of the simulation, the proximity of the failure is evident, with the maximum vertical displacement close to the structure axis and the occurrence of an uplift near the foot of the embankment. This movement was verified in field investigations carried out after the accident to identify the position of the breakwater berms (Sandroni et al., 2018).

4.1.2 Horizontal displacements

The horizontal displacements calculated in the model were compared with the results of the inclinometer installed in the instrumented station STA1, located on

Table 1. Geotechnical parameters determined for clay sublayers.

Sub-layer	General parameters				Mohr-Coulomb model				Soft Soil Creep model				
	γ_{sat} (kN/m ³)	k_{v0} (m/s)	e_0	c_k	E' (kPa)	ν'	$S_{u,VT}$ (kPa)	μS_u (kPa)	λ^*	κ^*	μ^*	K_o^{NC}	OCR
Clay 1	16.0	1.5×10^{-9}	1.7	0.85	5800	0.25	15.5	12.4	0.16	0.032	0.006	0.69	1.70
Clay 2			1.8	0.90	6000		15.5	12.4	0.16	0.032		0.69	1.55
Clay 3			1.9	0.95	6400		16.8	13.4	0.15	0.030		0.69	1.50
Clay 4			1.9	0.95	6700		19.3	15.4	0.15	0.030		0.65	1.50
Clay 5			1.8	0.90	7000		21.8	17.4	0.15	0.030		0.65	1.55
Clay 6			1.7	0.85	7200		23.0	18.4	0.15	0.030		0.65	1.55
Clay 7			1.6	0.80	7500		23.0	18.4	0.15	0.030		0.69	1.60

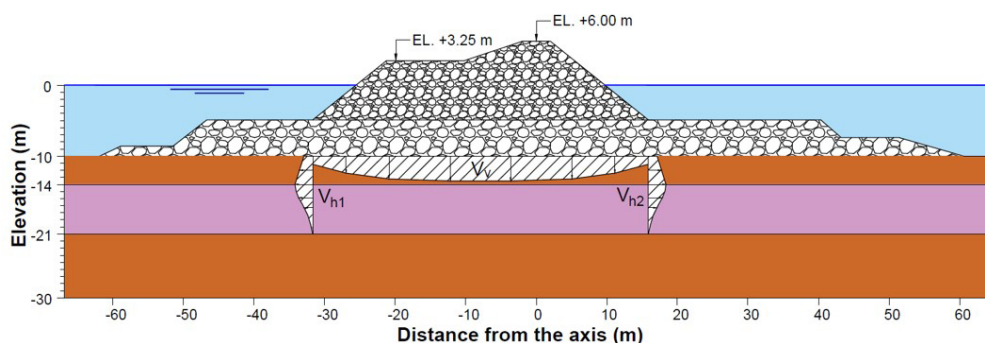


Figure 3. Schematic representation of the volumes of vertical and horizontal displacements.

the coast-side of the breakwater. Growing movements in this direction were noticed until the date of the failure. The comparison is shown in Figure 5, but the agreement between the numerical analysis and the instrumentation results was not satisfactory.

In the numerical analyses, the horizontal displacements calculated in the phases close to the moment of breakwater

rupture were closer to the measured ones. Some questions have been raised about these measurements with inclinometers.

There were uncertainties about the exact position of the inclinometer and the distance at which it was located and about the dates the measurements were taken. Additionally, this inclinometer tube was spiraled (Sandroni, 2016), so that the available displacement profiles were corrected.

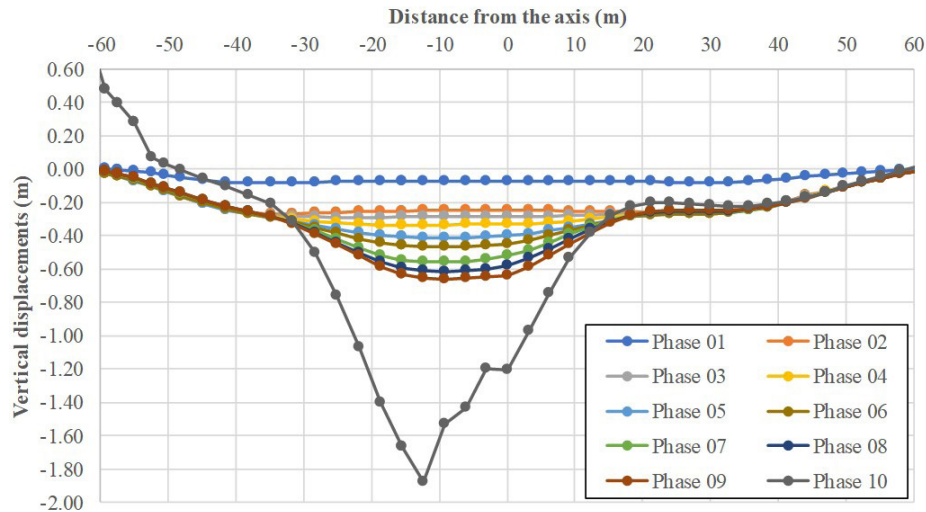


Figure 4. Vertical displacements at the base of the breakwater at the end of each loading phase.

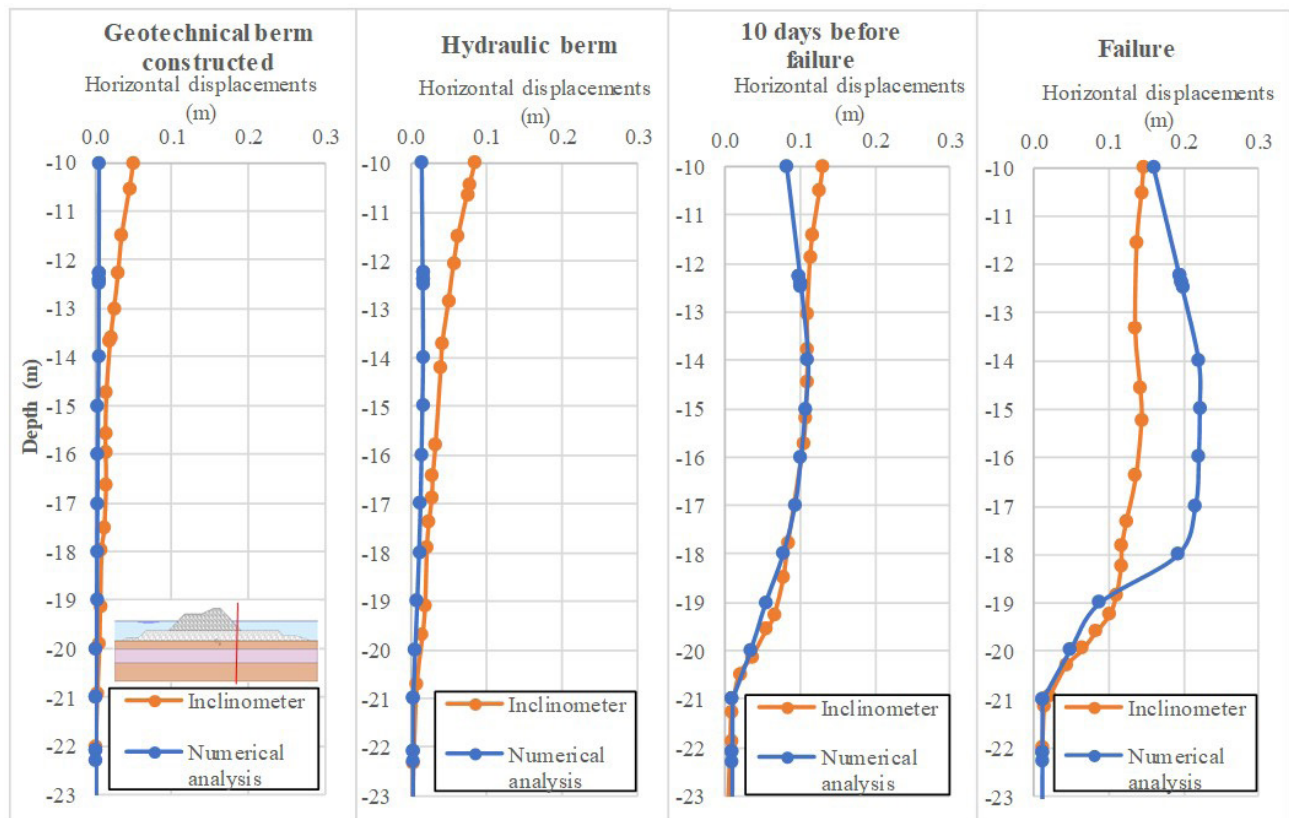


Figure 5. Profiles of horizontal displacements measured by the STA1 inclinometer and numerically calculated at different times for the TPS breakwater.

In the authors' opinion, the profile of inclinometer readings was anomalous for the configuration of the foundation and the geometry of the breakwater structure. The profile of horizontal displacements obtained in the numerical analyses seems to be more consistent with the behavior observed in other cases of embankments built on soft soils.

4.1.3 Pore pressures

The pore pressures calculated in the numerical simulation were consistent with the expected results, occurring an increase in pore pressures in the loading phases and dissipation in the consolidation phase of the geotechnical berm. This dissipation was greater along the draining boundaries and smaller in the central clay layers. Figure 6 shows excess pore pressure as a function of time. It is possible to observe that excess pore pressure was generated along the failure surface (green line), reducing the effective stresses acting on it.

4.1.4 Incremental shear strains

The failure mechanism can be followed by evaluating incremental shear strains ($\Delta\gamma_s$) in each of the loading phases of the model, as shown in Figure 7.

From these results, it is possible to observe that $\Delta\gamma_s$ was restricted only to the borders of the clay layer during the first phases of loading. The geometry of the breakwater, with the slopes of the hydraulic berm more inclined and a shorter distance from the foot to the end of the geotechnical berm, favored the development of a failure surface, caused by the concentration of shear deformations during the construction.

As of Phase 06, in which the hydraulic berm is 7.0 m high, the interpretation of the results indicates the formation of two potential failure surfaces. However, the magnitude of $\Delta\gamma_s$ is greater towards the side of the sea, as is the extent of the potential rupture surface.

In the last loading phase (Phase 10), the failure surface is well developed towards the sea. The failure surface calculated in the numerical simulation is similar to the surface verified in field investigations after failure of the structure.

However, the fact that it was observed the formation of two potential failure surfaces does not imply that shear strength was not mobilized in the rockfill. The analysis of the calculated effective stress path for a point in this material indicates that the maximum deviation stresses were mobilized (Figure 8a). Figure 8b presents the contours of relative shear stresses (τ_{rel}) given by the ratio between mobilized stresses (τ_{mob}) and maximum admissible stresses (τ_{max}) in the penultimate phase of the numerical simulation. It is possible to observe that, even before the failure, the relative stresses were equal to 1.0 in great part of the breakwater body.

4.1.5 Effective stress paths

Figure 9 presents the effective stress paths of some selected points, for all phases of the numerical simulation during the construction of the breakwater. The initial effective stress state is determined as a function of the unit weight, the buoyancy coefficient at rest and the *OCR* of the breakwater foundation materials.

In each graph are shown the Mohr-Coulomb failure envelope (in black), the critical state line CSL (in red) and the ellipse p_{eq} that defines the initial cap yield surface (in gray) of each point.

The effective stress paths follow the expected behavior according to the loading condition imposed by the construction of the breakwater. In general, the loading of the geotechnical berm generated effective stress increases like the stress paths imposed by triaxial compression tests with the generation of positive excess pore pressure.

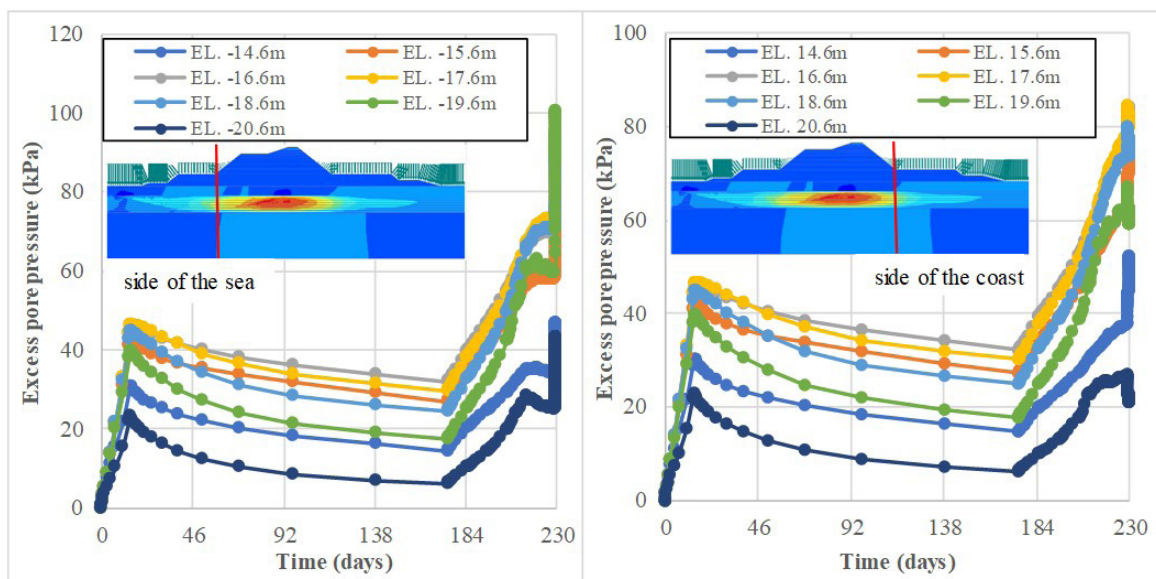


Figure 6. Excess pore pressure at different depths of the clay layer as a function of time.

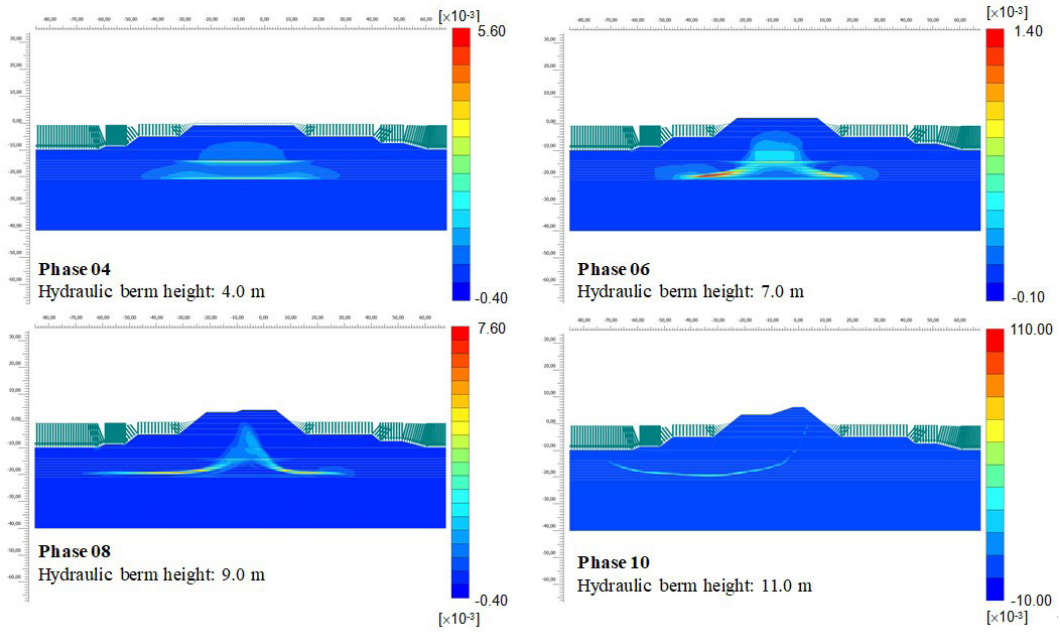


Figure 7. Contours of incremental shear strains in different phases of numerical simulation.

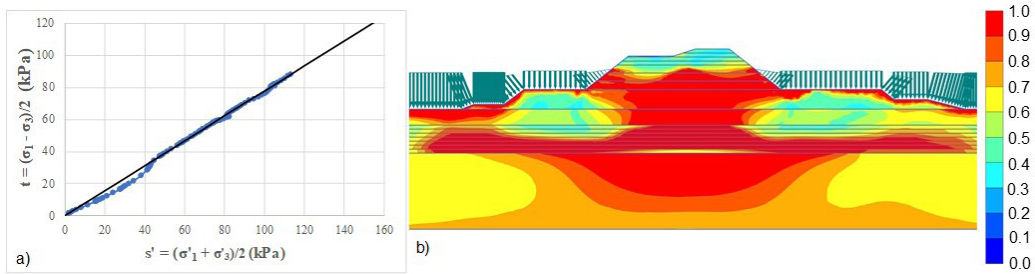


Figure 8. a) Effective stress path in the rockfill of the breakwater; b) contours of relative shear stress in Phase 09 in numerical simulation. The region in strong red indicates $\tau_{rel} = 1.0$.

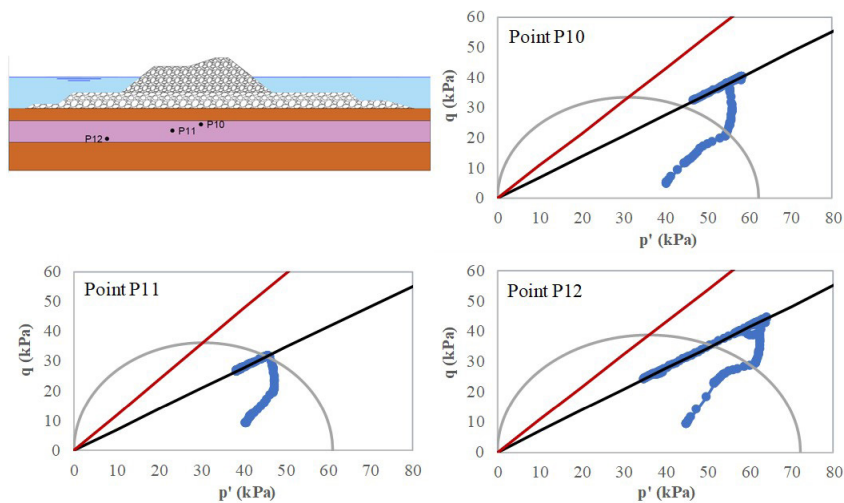


Figure 9. Effective stress paths at selected points in the clay layer located on the failure surface.

The first loading phases of the hydraulic berm already caused elastoplastic strains since the clay was already in the normally consolidation condition. After rupture, the effective stress paths followed the Mohr-Coulomb envelope towards the origin, indicating a strain softening behavior of the material, which represents a sensitivity of the material. This behavior, combined with the redistribution of shear stresses, is closely linked to the phenomenon of progressive failure in slopes (Leroueil et al., 2012).

4.1.6 Factors of safety

Figure 10 presents the undrained Factors of Safety (FoS) obtained in the numerical analyses as a function of the height of the breakwater, in each of the loading phases of the hydraulic berm. In addition to the results using the SSC model, where the soft clay was represented as an undrained material in terms of effective stresses, the clay layers were also modeled by the MC model in undrained condition in terms of total stresses.

In undrained analyses with the MC model with resistance gain (ΔSu), the FoS of the breakwater were greater than unity, with values in the last phase equal to 1.41 for analysis using Su from vane tests (VT) and 1.26 using corrected undrained strength ($\mu^* Su$). The results were higher than those obtained in a limit equilibrium analysis (Sandroni, 2016), with stress increases calculated by using pore pressures measured in piezometers installed a few meters from the breakwater axis, while in the present numerical analysis the variation of effective vertical stresses was determined under the axis of the structure. In addition, the resistance gains were calculated in each of the increment phases of the breakwater construction, generating in the last phase,

Su values higher than those used in stability analyses by the limit equilibrium method.

This may indicate that the clay of the foundation of the breakwater did not show resistance gain due to the consolidation process of the geotechnical berm, or that the resistance gain was much lower than that calculated in the traditional way, presenting a UU triaxial-like behavior.

Another hypothesis, suggested by Sandroni et al. (2018) would be that, despite this gain in strength, the sensitivity of the clay would cause a decrease in shear strength. According to Lacerda & Almeida (1995), the Sergipe clay would have sensitivity values from 4.0 to 6.0. This condition, verified in compression triaxial tests through the evaluation of the pore pressure parameter A after failure, is not simulated by the MC model.

In the analysis without resistance gain, considering or not the Bjerrum correction in Su , the FoS obtained were lower, and the values calculated for the last phase of the simulation were similar to those determined with the limit equilibrium method. For the analysis without correction, the FoS in the last phase was equal to 1.12, while for the one that used corrected Su , the failure occurred in the penultimate calculation phase, with a value equal to 1.00.

The analysis with the SSC model presented the most consistent results, with FoS values decreasing with the increase of the hydraulic berm until failure in the last loading phase, with a FoS equal to 0.99. The result differed considerably from the back analyses carried out by limit equilibrium.

This difference can be explained by the fact that the FEM generated higher values of excess pore pressure, mainly along the failure surface, which reduced the effective stresses and, consequently, the admissible shear stresses. Another

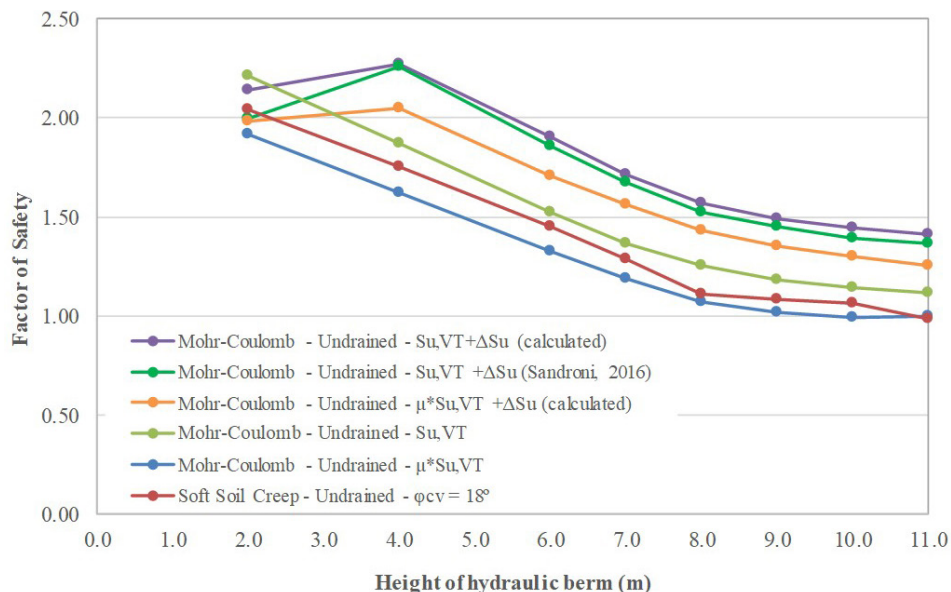


Figure 10. Factor of Safety obtained as a function of the height of the hydraulic berm for each analysis.

difference is the simulation of the strain softening behavior of the material after rupture, for the effective stress paths of the points located along the failure surface.

4.2 Volume method

Based on the displacement results obtained in the numerical simulation of the construction of the TPS breakwater, a stability assessment was carried out using the Volume Method (Sandroni et al., 2004) and comparing it with the FoS obtained in numerical stability analyses.

In the first loading phases of the berm, the β values varied between 1.0 and 1.5. After the outbreak of the rupture, an increase in β was observed due to the greater movements towards the side of the sea. Table 2 presents the displacement volumes and the calculation of $\Delta V_v / \Delta V_h$ for both sides of the breakwater (Figure 3), in each of the loading phases of the hydraulic berm.

Figure 11a shows calculated $\Delta V_v / \Delta V_h$ related to the embankment height of the hydraulic berm. It is possible to observe that, in the first loading phases of the hydraulic berm, the ratio $\Delta V_v / \Delta V_h$ is lower for the side of the coast when compared to the side of the sea, where the rupture occurred.

A comparison was also made between the results obtained by the Volume Method, for the side of the sea and the FoS obtained in the numerical simulation using the SSC model. Figure 11b shows, on the left vertical axis, the values of the FoS and, on the right vertical axis, the

values of the ratio $\Delta V_v / \Delta V_h$ as a function of the height of the hydraulic berm.

From Phase 05 (height of the hydraulic berm equal to 6.0 m), the value of $\Delta V_v / \Delta V_h$ on the side of the sea showed a sharp decrease. Both curves kept below the range of $\Delta V_v / \Delta V_h = 3.0$ until the penultimate berm increment. In the last phase of the simulation, when the rupture was triggered towards the side of the sea, it occurred large horizontal displacements, taking the ratio between the displacement volume variations to values below 1.0. The ratio $\Delta V_v / \Delta V_h = 3$, as an indicator of an unstable condition, occurred when the corresponding factor of safety was $FoS = 1.29$ determined from the numerical analysis (Figure 10). For the side of the coast, however, there was an increase of $\Delta V_v / \Delta V_h$ to values greater than 3.0.

5. Conclusion

The numerical analysis of the construction of the original TPS breakwater aimed to better understand the mechanisms that led to the failure of the structure, using constitutive soil models and other finite element tools not available at the time of the accident. In this way, the results obtained in this research can be considered a contribution, since the main aspects of the problem were examined in the analyses, in terms of displacements, deformations, pore pressures and the stability of the structure itself. A numerical analysis considering the redesigned TPS breakwater, constructed in the early 1990s, was presented by (Brugger et al., 1998).

Table 2. Displacement volumes and the calculation of $\Delta V_v / \Delta V_h$ for both sides of the breakwater.

Phase	V_{hl} (m ³ /m)	V_{h2} (m ³ /m)	β	V_v (m ³ /m)	V_{vl} (m ³ /m)	V_{v2} (m ³ /m)	ΔV_{hl}	ΔV_{h2}	ΔV_{vl}	ΔV_{v2}	$\Delta V_{vl} / \Delta V_{hl}$	$\Delta V_{v2} / \Delta V_{h2}$
Phase 03	0.311	0.214	1.45	13.497	7.640	5.857	0.160	0.152	0.828	0.634	5.182	4.167
Phase 04	0.506	0.398	1.27	15.382	8.707	6.675	0.194	0.184	1.067	0.818	5.496	4.457
Phase 05	0.825	0.688	1.20	17.928	10.148	7.780	0.319	0.290	1.440	1.104	4.515	3.802
Phase 06	1.149	0.945	1.22	19.622	11.107	8.515	0.325	0.256	0.959	0.736	2.954	2.869
Phase 07	2.070	1.481	1.40	22.251	12.595	9.656	0.921	0.537	1.488	1.141	1.617	2.126
Phase 08	2.420	1.820	1.33	23.943	13.553	10.390	0.351	0.339	0.958	0.734	2.732	2.165
Phase 09	2.761	2.185	1.26	25.523	14.447	11.076	0.340	0.365	0.894	0.686	2.628	1.881
Phase 10	23.68	4.367	5.42	48.959	27.713	21.246	20.915	2.182	13.266	10.170	0.634	4.661

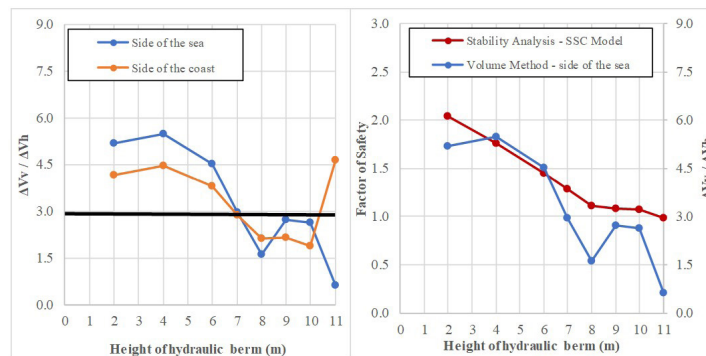


Figure 11. (a) $\Delta V_v / \Delta V_h$ as a function of the height of the hydraulic berm; (b) FoS and $\Delta V_v / \Delta V_h$ as a function of the height of the hydraulic berm.

From the analysis, it was possible to point out the hypothesis that the pressures acting on the clay layer at the moment of failure were higher than those adopted in former back analyses by the limit equilibrium method based on the readings of the piezometers.

The use of the SSC model allowed simulating a strain softening behavior, with loss of resistance after the peak. This property of geotechnical materials is important for the stability analysis, because when associated with the redistribution of shear stresses along the failure surface, it can cause a progressive rupture.

Analyses using the MC model, with different S_u values, resulted in FoS similar to those obtained by the limit equilibrium method. The most plausible interpretation of these results indicates that, despite the gain in strength due to the consolidation of the clay layer, its sensitive behavior led to a mobilized shear strength much lower than the expected peak.

Although shear deformations and horizontal displacements of significant magnitude were observed for both sides of the breakwater, the shared failure hypothesis could not be properly demonstrated. The analysis of the stress paths and the relative shear stresses in the rockfill indicate that the shear resistance was mobilized in the rockfill body.

The analyses also indicated that the empirical Volume Method, originally proposed for monitoring works with field instrumentation, indicated that when the potentially unstable condition was reached ($\Delta V_v / \Delta V_h = 3$), the corresponding undrained factor of safety was $FoS = 1.29$ determined from the finite element analysis. Other applications of the Volume Method found in the literature, either applying results from field instrumentation (Cobe, 2017; Sandroni et al., 2018; Cordeiro, 2019) or numerical simulation (Dienstmann, 2011) indicate that this empirical method can be a useful tool for monitoring embankment constructions. In the authors' knowledge there is no published results relating the variation of the factor of safety against the volume ratio ($\Delta V_v / \Delta V_h$) as investigated in the present research. A generalization of this correspondence would imply the analysis of many other practical cases, including the verification of the stable and unstable ranges proposed by Sandroni et al. (2004).

Acknowledgements

To PUC-Rio and professors Sandro Sandroni and Willy Lacerda. This research was carried out with the support of the Coordenação de Aperfeiçoamento de Pessoal de Nível Superior – Brazil – Brazil (CAPES) – Financing Code 001.

Declaration of interest

The authors have no conflicts of interest to declare. All co-authors have observed and affirmed the contents of the paper and there is no financial interest to report.

Authors' contributions

Pedro Oliveira Bogossian Roque: conceptualization, data curation, writing – original draft. Celso Romanel: methodology, supervision, writing – review. Celso Antero Ivan Salvador Villalobos: validation, writing – review. Jackeline Castañeda Huertas: conceptualization, methodology, validation.

Data availability

The datasets generated analyzed in the course of the current study are available from the corresponding author upon request.

List of symbols

c_k	Change in permeability coefficient
e_0	Initial void ratio
C_c	Compression index
C_s	Swelling index
E'	Young's modulus
FoS	Factor of safety
K_0^{NC}	Coefficient of earth pressure at rest for normally consolidated soils
OCR	Overconsolidation ratio
Su_{VT}	Undrained shear strength obtained by vane tests
V_h	Volume of horizontal displacements
V_v	Volume of vertical displacements
β	Asymmetry parameter, ratio between the volumes of horizontal displacements
γ_{sat}	Saturated unit weight
$\Delta\gamma_s$	Incremental shear strain
κ^*	Modified swelling index (Soft Soil model parameter)
λ^*	Modified compression index (Soft Soil model parameter)
μ	Bjerrum correction factor
μ^*	Modified creep index (Soft Soil Creep model parameter)
τ_{max}	Maximum admissible shear stress
τ_{mob}	Mobilized shear stress
τ_{rel}	Relative shear stress
ν'	Poisson's ratio
ϕ_{cv}	Critical-void friction angle

References

- Brugger, P.J. (1996). *Análise de deformações em aterros sobre solos moles* [Doctoral thesis]. Instituto Alberto Luiz Coimbra de Pós-Graduação e Pesquisa de Engenharia, Universidade Federal do Rio de Janeiro (in Portuguese).
- Brugger, P.J., Almeida, M.S.S., Sandroni, S.S., & Lacerda, W.A. (1998). Numerical analysis of the breakwater construction of Sergipe Harbour, Brazil. *Canadian Geotechnical Journal*, 35(6), 1018-1031. Retrieved in May 15, 2023, from <https://cdnscepub.com/doi/10.1139/t98-063>

- Bjerrum, L. (1973). Problems of soil mechanics and construction on soft clays. In *Proceedings of the 8th International Conference on Soil Mechanics and Foundation Engineering* (Vol. 3, pp. 111-159). Moscow.
- Cobe, R.P. (2017). *Behavior of an embankment constructed on a soft clay foundation and its influence on the adjacent piles* [Master's dissertation, Pontifícia Universidade Católica do Rio de Janeiro]. Pontifícia Universidade Católica do Rio de Janeiro's repository (in Portuguese). <https://doi.org/10.17771/PUCRio.acad.36574>.
- Cordeiro, R.F. (2019). *Avaliação do comportamento de aterro executado sobre depósito de argila mole na rodovia BR 470 em Gaspar/SC* [Master's dissertation, Universidade Federal de Santa Catarina]. Universidade Federal de Santa Catarina's repository (in Portuguese). <https://repositorio.ufsc.br/handle/123456789/215088>.
- Dienstmann, G. (2011). *Projeto interativo dos molhes da Barra do Rio Grande – RS* [Doctoral thesis, Universidade Federal do Rio Grande do Sul]. Universidade Federal do Rio Grande do Sul's repository (in Portuguese). <http://hdl.handle.net/10183/32005>.
- Geoprojetos. (1992). *Terminal Portuário de Sergipe – Relatório R-290592-137-39*. Geoprojetos Engenharia Ltda.
- Lacerda, W.A., & Almeida, M.S.S. (1995). Engineering properties of regional soils: residual soils and soft clays – State-of-the-art lecture. In *Proceedings of the 10th Panamerican Conference on Soil Mechanics and Foundation Engineering* (Vol. 4, pp. 161-176). Guadalajara.
- Ladd, C.C., & Lee, S.M. (1993). *Engineering properties of sergipe clay: TPS Progress Rept. No. 4. Research Rept R93-07*. MIT Department of Civil and Environmental Engineering.
- Leroueil, S., Locat, A., Eberhardt, E., & Kovacevic, N. (2012). *Landslides and engineered slopes: protecting society through improved understanding*. CRC Press. Progressive failure in natural and engineered slopes, pp. 31-46.
- Ribeiro, L.F.M. (1992). *Ensaio de laboratório para determinação das características geotécnicas da argila mole de Sergipe* [Master's dissertation]. Pontifícia Universidade Católica do Rio de Janeiro (in Portuguese).
- Sandroni, S.S. (2016). *Willy Lacerda: doutor no saber e na arte de viver*. Geobruigg. Novo Projeto do quebra-mar de Sergipe depois da ruptura durante a construção, pp. 326-336.
- Sandroni, S.S., Brugger, P.J., Almeida, M.S.S., & Lacerda, W.A. (1997). Geotechnical properties of Sergipe clay. In *Proceedings of the International Symposium on Recent Developments on Soil and Pavement Mechanics*, Rio de Janeiro: CRC Press, 271–277.
- Sandroni, S.S., Lacerda, W.A., & Tassi, M. (2018). Landslide during construction of a rockfill breakwater in the coast of Sergipe, Brazil. In *Proceedings of the International Symposium on Field Measurements in Geomechanics*, Rio de Janeiro. Session 3.
- Sandroni, S.S., Lacerda, W.A., & Brandt, J.R.T. (2004). Método dos volumes para controle de campo da estabilidade de aterros sobre argilas moles. *Solos e Rochas*, 27, 25-35.
- Schnaid, F., & Odebrecht, E. (2012). *Ensaio de campo e suas aplicações à engenharia de fundações* (2. ed.) Oficina de Textos.